PAPER

Check for updates

Shear-aligned graphene oxide nanosheets incorporated PVDF composite membranes for selective dye rejection with high water flux†

Sk Safikul Islam, [a] Theres Jose,[a] Asiful Hossain Seikh,[b] Mohammad Rezaul Karim,[b] Ibrahim A. Alnaser*[b] and Suryasarathi Bose *[a]

Membrane technology is crucial in addressing water pollution challenges, particularly in removing dyes from wastewater. This study presents a novel approach to fabricating shear-aligned graphene oxide (GO) nanosheets incorporated polyvinylidene fluoride (PVDF) membranes for achieving exceptional dye rejection efficiency while maintaining high water flux. The membranes were prepared by dispersing graphene oxide within a PVDF matrix and subsequent subjection to shear alignment techniques. Shear and flow-induced alignment were explored to achieve precise and controlled alignment of graphene oxide flakes within the PVDF matrix. The resulting membranes exhibited enhanced structural integrity and optimized molecular packing of PVDF and GO, enabling them to selectively reject dyes while allowing efficient water permeation. The fabricated membranes were extensively characterized using appropriate testing methods. The results demonstrated that the shear-aligned GO sheets infused PVDF composite membranes exhibited outstanding dye rejection (96–99%) performance, surpassing conventional membranes while maintaining high water flux. This innovative membrane fabrication approach holds significant promise for advanced water treatment applications, offering a sustainable solution for selective dye removal and efficient water purification.

1 Introduction

Water scarcity is a pressing global issue that poses significant challenges to human well-being, environmental sustainability, and economic development. With increasing population growth, industrialization, and climate change, the demand for freshwater resources has surpassed the available supply in many regions worldwide.[1-3] This scarcity of water resources has far-reaching consequences, affecting agriculture, industry, and the overall quality of life. Membrane-based water treatment systems have emerged as a promising solution due to their ability to selectively separate contaminants from water. Traditional membranes often suffer from limitations such as low water flux, fouling, and inefficient removal of specific contaminants, reducing water quality and increasing energy consumption. Therefore, there is a need to develop advanced membrane materials that can effectively address these limitations and contribute to sustainable water management.

In recent years, graphene oxide (GO) and other two-dimensional (2D) materials have gained significant attention for their potential applications in membrane technology and water treatment.[4-8] Graphene oxide-based 2D materials offer tremendous potential for membrane technology and water remediation applications. Their unique physicochemical properties, including large surface area, tunable pore size, and selective interactions with contaminants, enable the development of advanced membranes with improved water flux and selective pollutant removal.[9-16] novel "posterior" interfacial polymerization (p-IP) strategy has been introduced to construct a customized polyamide (PA) network *in situ* within an ultrathin GO membrane, effectively repelling metal ions.[17] Further research and development efforts in this field hold promise for addressing water scarcity, improving water quality, and advancing sustainable water management practices.

PVDF is a highly durable and mechanically robust polymer. PVDF is a critical component in GO-based mix matrix membranes due to its enhanced mechanical strength, chemical compatibility, hydrophobicity, fouling resistance, tunable porosity, and compatibility with GO dispersion.[18-22] These properties contribute to the overall performance and reliability of the membranes, enabling effective water treatment processes such as selective pollutant removal and enhanced water flux.

Various strategies have been employed to incorporate GO-based 2D materials into membranes. GO can be blended with polymers such as polyvinylidene fluoride (PVDF),[23] polysulfone (PSf),[24] or polyamide (PA)[25] to form composite membranes. The

[a]*Department of Materials Engineering, Indian Institute of Science, Bangalore-560012, Karnataka, India. E-mail: sbose@iisc.ac.in*

[b]*Center of Excellence for Research in Engineering Materials (CEREM), King Saud University, P.O. Box 800, Al-Riyadh 11421, Saudi Arabia. E-mail: ianaser@ksu.edu.sa*

† Electronic supplementary information (ESI) available. See DOI: https://doi.org/10.1039/d4ra04147j

dispersion of GO in the polymer matrix enhances the membranes' mechanical strength, chemical stability, and anti-fouling properties. Graphene oxide-doped polyvinylidene fluoride (PVDF) membranes have shown great potential in water treatment applications.[26–28] Graphene oxide, a two-dimensional nanomaterial with exceptional mechanical strength and chemical stability, can be incorporated into PVDF membranes to enhance their performance. The unique properties of graphene oxide, such as its high surface area, excellent selectivity, and tunable pore size, make it an ideal candidate for improving water treatment processes.[29–32]

Herein, we intercalated 2D GO materials into PVDF dope solutions and cast the membrane with a 300 μm doctor's blade. In order to investigate the morphological and physicochemical properties of GO and GO@PVDF membranes, a range of characterization techniques were used. Incorporating GO into PVDF membranes significantly improved water flux while maintaining selectivity for cationic and anionic dyes in nanofiltration (NF) applications. The membrane also exhibits lower salt rejection performance, particularly for Na_2SO_4, with a rejection rate of 48%. However, the membrane exhibits outstanding stability over a broad pH range, demonstrating its robustness and ability to maintain performance under harsh conditions. This enhancement in performance highlights the effectiveness of GO@PVDF membranes compared to pristine prGO membranes.

2   Experimental section

2.1   Materials and methods

Polyvinylidene fluoride (PVDF) (Mw = 440 000 g mol^{-1}) was obtained from Arkema. Graphite and N,N-dimethylformamide (DMF), 99.0% were procured from Sigma Alrich. Methylene blue (MB), congo red (CR), methyl orange (MO), rhodamine blue (RB) dyes, potassium permanganate ($KMnO_4$, 99.9%), sulfuric acid (H_2SO_4, 98%) phosphoric acid (H_3PO_4, 99%) hydrochloric acid (HCl, 35–38%), hydrogen peroxide (H_2O_2, 30%), sodium sulfate (99%), sodium chloride (99.90%), acetone, ethanol were collected from a local vendor. All the chemicals and obtained materials were used without additional processing or purification.

2.2   Graphene oxide (GO) synthesis

According to reports in the literature, the modified Hummers' method is used to synthesize GO in a highly acidic medium.[33] Briefly, 68 ml of a 10 : 58 volume ratio of H_3PO_4 and H_2SO_4 are combined with 1 g of powdered graphite. After adding 6 g of $KMnO_4$, the mixture was subjected to a magnetic stirrer at 0–4 °C for a duration of one hour. It is maintained and stirred for three days at room temperature to achieve complete oxidation. The reaction is stopped, and the excess $KMnO_4$ is neutralized by adding H_2O_2 dropwise. The unreacted graphite is fully removed using 1 N HCl and DI water in that order. The GO is then isolated by centrifugation at 8000 rpm. The resulting GO is dried at room temperature under vacuum conditions, yielding approximately 60%.

2.3   Fabrication of SAGO@PVDF membrane

To prepare a dope solution, 7.5 ml of DMF solvent was added to 30 wt% of PVDF in a 50 ml beaker. The components were stirred continuously at 80 °C until a consistent bubble-less solution was obtained. To this, 200 mg of GO in 2.5 ml DMF was added. The solution was stirred in a hot plate until a homogeneous and uniformly mixed dope solution was obtained. The membranes were cast by using a 300 μm doctor blade, and a speed of 7–8 cm s^{-1} was set in an automatic film applicator for casting the membranes onto a glass plate. Before performing experiments, the constructed membranes were cleaned and rinsed with ultrapure water before performing any experiments. The fabricated membranes were termed SAGO@PVDF and yielded 90%. GO sheets were shear aligned in a particular direction, mainly responsible for high rejection performance (Fig. 1).
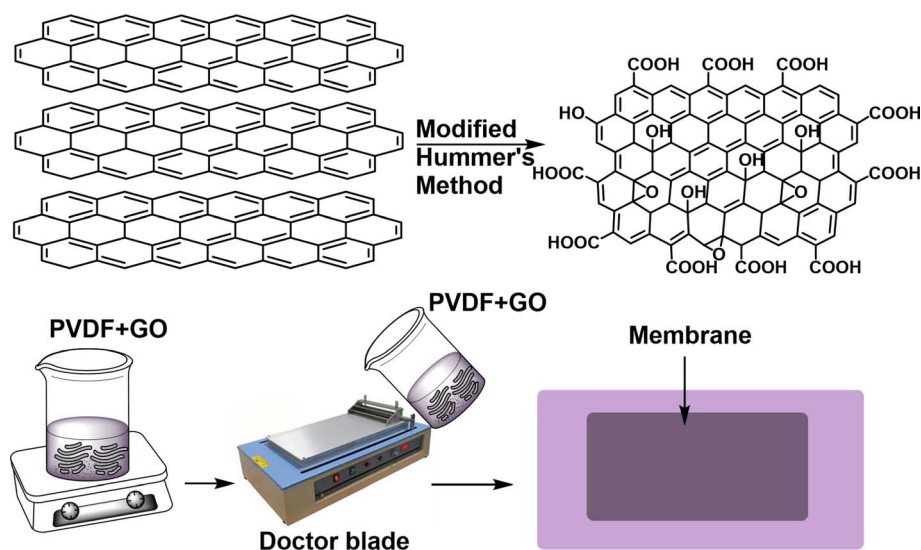

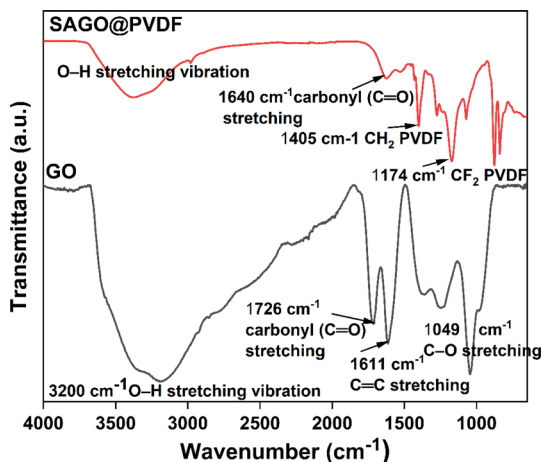Fig. 1   Schematic representation showing the preparation process of (a) GO (b) SAGO@PVDF membrane.

Fig. 2 FTIR spectra of GO and SAGO@PVDF membrane.

3 Results and discussion

Fourier transforms infrared (FTIR) spectroscopy was used to examine the functional groups found in graphene oxide (GO) and graphene oxide incorporated polyvinylidene fluoride membrane (SAGO@PVDF) in Fig. 2. At specific wavenumbers, especially 1044 cm^{-1}, 1612 cm^{-1}, 11 721 cm^{-1}, and 3200 cm^{-1}, graphene oxide displayed different absorption peaks.[34] These peaks represent the C–O, C–C, carbonyl (C–O) stretching and O–H stretching vibration respectively. Two additional peaks were found at 1405 cm^{-1} and 1174 cm^{-1} after graphene oxide was added to the PVDF matrix for developing the SAGO@PVDF membrane corresponding to the CH_2 and CF_2 groups of PVDF. These extra peaks show that the PVDF matrix successfully integrated the graphene oxide particles according to their existence.

The structural and d-spacing alterations in the graphene oxide (GO) powders and the composite with graphene oxide added to PVDF (SAGO@PVDF) were examined using X-ray diffraction (XRD) analysis. The XRD pattern confirmed the successful production of the GO particles, which exhibited

a noticeable diffraction peak at 10.54° (Fig. 3), representing the oxidized graphitic peak. The corresponding interplanar spacing (d) for GO measured 0.84 nm, which decreased to 0.76 nm in the final SAGO@PVDF membrane. An additional peak at 20.84° in the XRD pattern was seen after combining the PVDF polymer with GO particles, indicating the PVDF is semi-crystalline.[20] Thus, this peak and the typical GO peak suggest that GO was successfully incorporated into the PVDF matrix, preserving the integrity of the nanosheets within the matrix. This integration enhances the performance and stability of the membrane.

The surface chemistry of GO particle and SAGO@PVDF membranes were further characterized by X-ray photoelectron spectroscopy (XPS) in Fig. 4. The outcomes of XPS investigations suggest that the primary components of GO are carbon and oxygen. The confirmation of the presence of 1S oxygen (1S O) on the surface of GO is also supported by the presence of a peak at 532.08 eV. One addition peak was observed for SAGO@PVDF membranes, along with carbon and oxygen, confirming the presence of 1S F (688.08 eV), further suggesting that GO and PVDF moiety successfully mixed properly.[4,21] After deconvolution, four peaks for the sp2C/sp3C, C–O, –COOH, and –CF_2 were
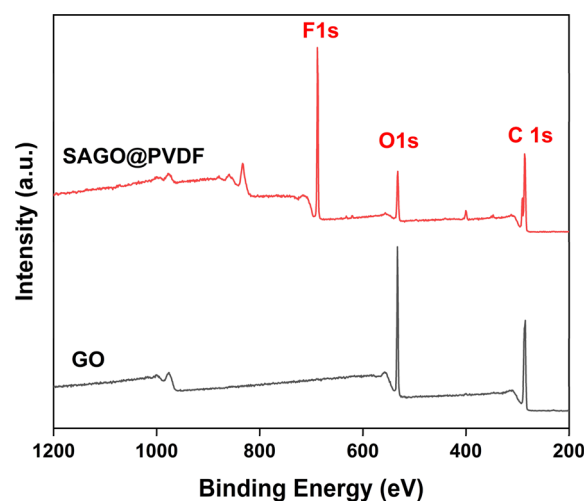

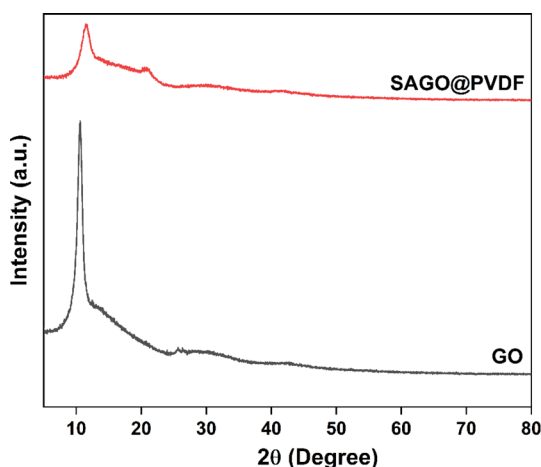Fig. 4 XPS survey spectra of GO and SAGO@PVDF membrane.
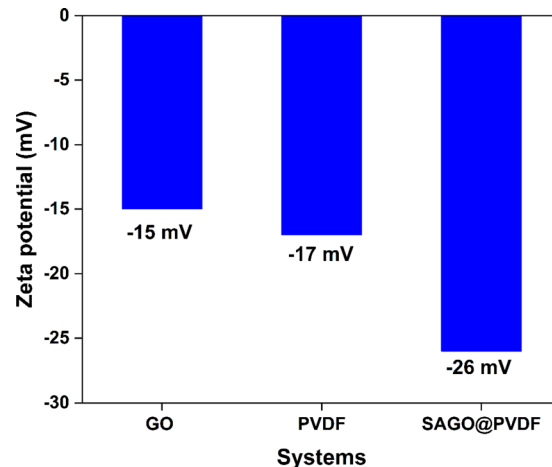

Fig. 3 XRD data of GO and SAGO@PVDF membrane.

Fig. 5 Zeta potential of GO, PVDF, and SAGO@PVDF membrane.

observed at 283.3, 285, 287.12, and 289.34 eV for the 1s C of SAGO@PVDF.

The zeta potential of the SAGO@PVDF membrane was evaluated using an Anton Paar Surpass 3 analyzer. Graphene oxide (GO) powder zeta potential was determined to be −15 mV, as shown in Fig. 5, similar to previous studies.[4] The PVDF membrane exhibited a zeta potential of −17 mV. On the other hand, the mixed matrix SAGO@PVDF membrane displayed an elevated negative zeta potential, measured −26 mV.[35] This increase in the negative zeta potential can be attributed to the SAGO@PVDF membrane's carboxyl/hydroxyl and fluoride groups. This negatively charged moiety on the surface of the membrane significantly impacts how effectively separation performance functions and how essential it is. These results show the impact of surface charge in affecting separation achievement and highlight the importance of zeta potential in membrane characterization.

The surface morphology and cross-section of the SAGO@PVDF membrane were studied using scanning electron microscopy (SEM). The surface of SAGO@PVDF composite membranes exhibits continuous rough wavy type, as shown in Fig. 6a and b, and the cross-section view reveals the thickness of 150 μm formed by shear aligning GO sheets to the PVDF matrix.[22,36] The defects and cavities on the surface of the membrane were not through, and it did not affect the membrane performance. We predict from SEM analysis that the shear aligns graphene sheets in PVDF enable water transport at high pressure while maintaining their mechanical strength, the cause of the SAGO@PVDF membrane's superior performance. The EDAX spectra of SAGO@PVDF (Fig. 6c) indicate the presence of carbon, oxygen, and fluorine elements.

The hydrophobicity or hydrophilicity of the membrane is a crucial factor in determining the characteristics of the fabricated membrane and, ultimately, its performance. A membrane would be more resistant to fouling problems if it were more hydrophilic, which is a serious danger to the current commercial membranes. A hydration layer that forms on top of the membrane surface is encouraged by hydrophilicity, which prevents biofouling. Therefore, hydrophilic membranes are currently required. A crucial method for determining a membrane's hydrophobicity or hydrophilicity is to measure its water contact angle. When SAGO@PVDF membranes were used, the water contact angle substantially decreased to 66°, as opposed to neat PVDF membranes, which had a water contact angle of around 94° (Fig. 7).[37] Because of this, the SAGO@PVDF membranes were virtually hydrophilic. The inclusion of GO particles into the PVDF matrix made the SAGO@PVDF
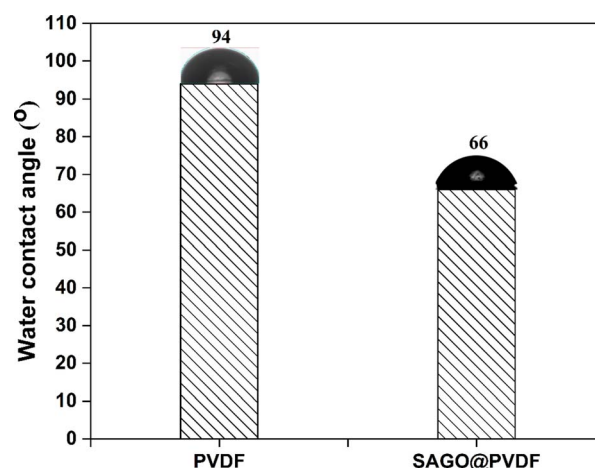

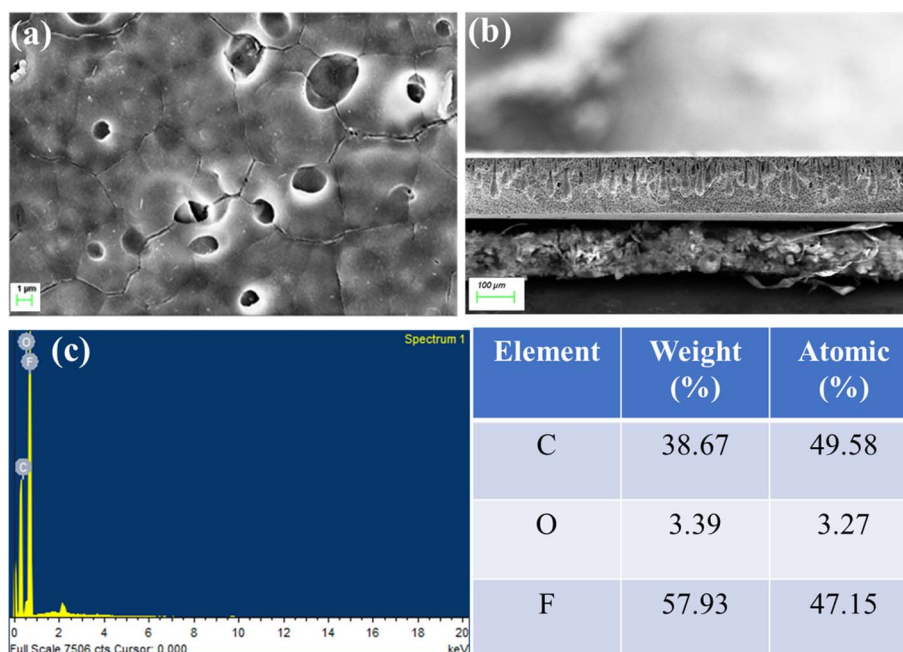Fig. 7 Water contact angle values for GO and SAGO@PVDF membrane.

Element	Weight (%)	Atomic (%)
C	38.67	49.58
O	3.39	3.27
F	57.93	47.15

Fig. 6 SEM Surface image (a) and cross-section image (b) and (c) EDAX spectra of SAGO@PVDF membrane.
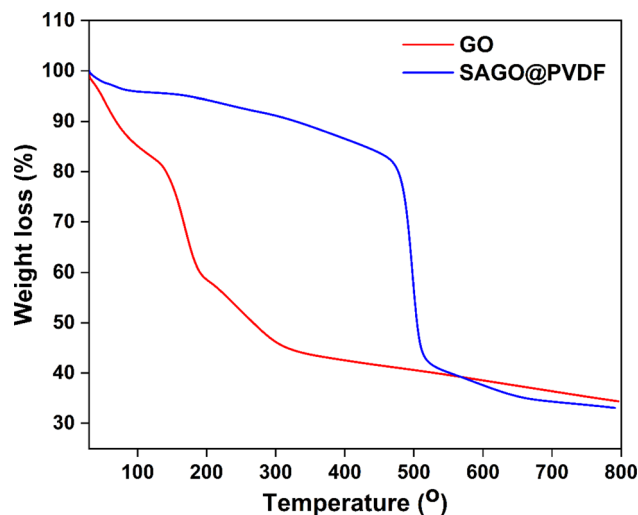
Fig. 8 TGA profiles of GO and SAGO@PVDF membrane demonstrating the thermal degradation behavior.
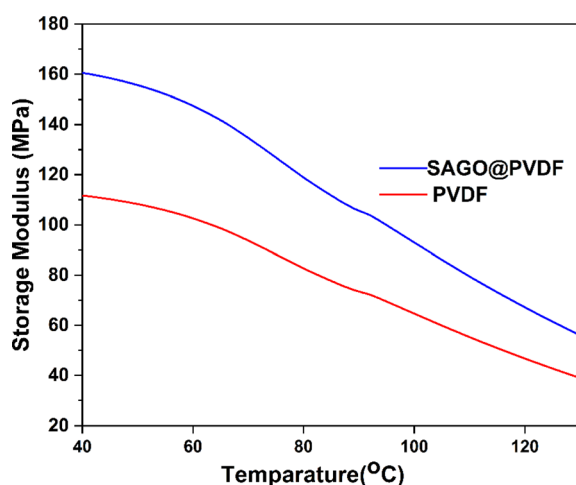

Fig. 9 DMA curves depicting the mechanical integrity of PVDF *vs.* SAGO@PVDF membranes.

membranes fundamentally hydrophilic in nature. The hydrophilic nature was introduced into the membrane architecture by the functional groups contained in GO (–OH, –COOH, and epoxide), which is what caused the contact angle value to decrease drastically. This membrane's hydrophilic surface would make it easier for a hydration layer to form, preventing fouling.

To further elucidate phase formation and investigate the structural improvements achieved through the formation of ordered phases, Small-Angle X-ray Scattering (SAXS) was conducted (Fig. S3†). The scattering vector, q ($q = 2\pi/d = 4\pi \sin \theta/\lambda$), was employed to evaluate the structural advancements in the SAGO@PVDF membrane. The required structural information for the SAGO@PVDF membrane was obtained from the Lorentz-corrected Kratky plot ($I \times q^2$ *vs.* q). The SAXS data revealed intense sharp peaks at 0.042 nm^{-1}, indicating the nematic phase of GO in the final membrane. Additionally, the shear alignment achieved during the casting of the SAGO@PVDF membrane resulted in the appearance of two additional peaks near 0.091 nm^{-1} and 0.145 nm^{-1}, signifying the presence of a lamellar phase. These observations lead to the conclusion that the high-order nematic and lamellar phases in the SAGO@PVDF membrane are attributable to the incorporation of GO nanosheets, with PVDF further stabilizing these phases within the membrane.[38,39]

The thermal stability of GO particle and SAGO@PVDF membrane was analyzed by the thermogravimetric analysis, TA Q500 instrument. The thermal degradation behaviour of the GO and SAGO@PVDF membranes is shown in Fig. 8. The GO particle has a two-step deterioration trend (at 120–145 °C and 190–220 °C). On the other hand, the final degradation temperature of the SAGO@PVDF membrane is approximately 470 °C, which is much higher than that of GO.[40] After the GO was incorporated into the PVDF matrix, filling in the pores. This significant increase in the thermal degradation values indicates much higher stability of SAGO@PVDF membranes.

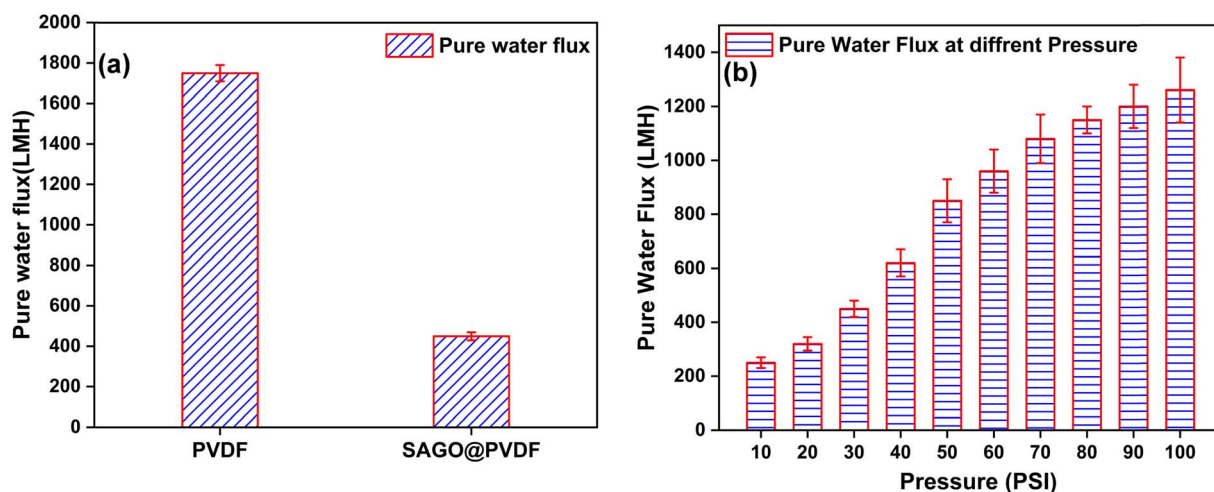The mechanical strength and integrity of SAGO@PVDF membranes and the impact of GO nanosheets on these

Fig. 10 (a) Pure water flux of PVDF and SAGO@PVDF membrane, (b) pure water flux at different pressure of SAGO@PVDF membrane.

membranes were assessed using a dynamic mechanical analysis (DMA). The storage modulus *vs.* temperature profiles for PVDF and SAGO@PVDF membranes are shown in Fig. 9. The graphs clearly show that adding shear-aligned GO sheets to the PVDF matrix significantly increases the storage modulus of the membranes. In particular, the storage modulus has increased significantly, from 112 MPa to about 162 MPa.

3.1 Rejection performance of the SAGO@PVDF membrane

The measurement of pure water flux was conducted utilizing an internally used cross-flow setup. The SAGO@PVDF membranes used to monitor water flux were 150 μm thick. Compared to the neat PVDF membrane (1750 LMH), pure water flux for graphene oxide doped PVDF mixed matrix membrane shows a 450 LMH flux. When graphene oxide was added to the PVDF membrane, we saw a substantial decrease in the flux of pure water. Water molecules cannot pass through the PVDF membrane when graphene oxide is added, possibly due to modifications to the membrane's structure or pore size distribution. According to Fig. 10, the assessment of pure water flux for SAGO@PVDF membranes at a range of applied pressures, ranging from 10 psi to 100 psi. With an increase in applied pressure, pure water flux rises linearly. The performance of the membrane was notably superior to that of the majority of commercially available NIPS membranes, exhibiting flux values within the range of 450 LMH at 100 psi.[32] The orderly alignment of GO sheets and the density of oxygen-containing molecules are responsible for the improved water penetration in the SAGO@PVDF membrane. High hydrophilicity was observed in the current investigation

due to changes in the surface characteristics and chemical composition of GO sheets after the membrane fabrication. We think the increased water flux in the SAGO@PVDF membrane was caused by the frictionless water transport provided by the slip-flow mechanism. Therefore, we believe that the combined effects of hydrophilicity and highly organized graphene nano-channels in the membrane cause the increased water flux of the SAGO@PVDF membrane.[41]

Methylene Blue (MB) and Rhodamine B (RB), a cationic dye; Congo Red (CR) and Methyl Orange (MO), both classified as anionic dyes, were selected as the model dye foulants. Fig. 11a
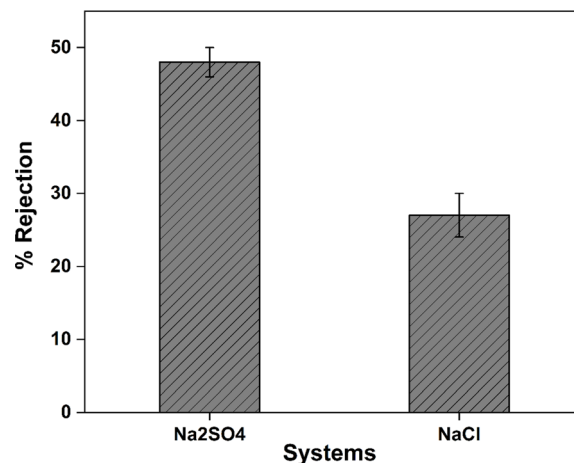

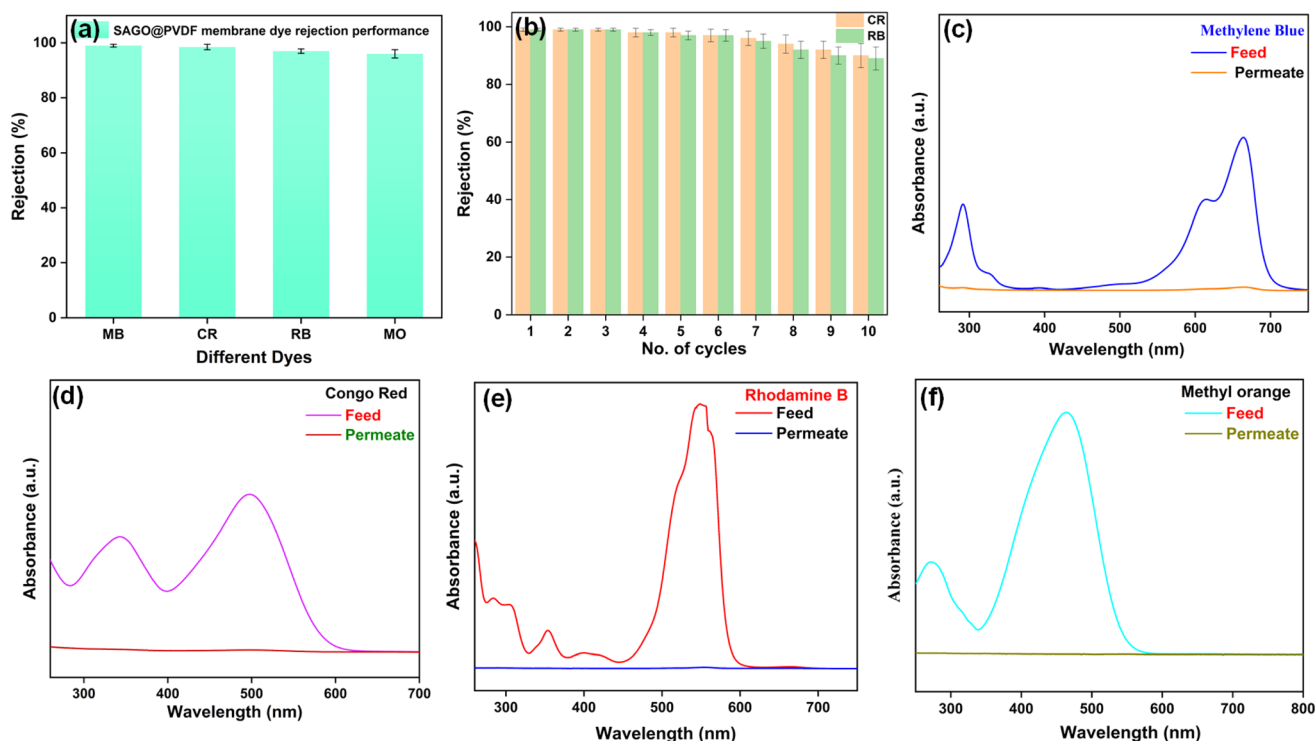Fig. 12   Salt ion rejection of SAGO@PVDF membrane.

Fig. 11   (a) Rejection of dye of SAGO@PVDF membrane (b) long-term dye rejection performance of SAGO@PVDF membrane with Congo Red (CR) and Rhodamine B as the model foulants, (c–f) U.V. spectrum of dyes, (a) M.B., (b) C.R., RB, and MO (top) feed solution, (bottom) filtrate.

Table 1 Comparison of the rejection performance (dye/salt) of SAGO@PVDF membranes with other PVDF-based membranes

Membrane	Flux	Dye	Salts	Ref.
PVDF/GO/TiO$_2$ membrane	49	92.61	—	43
PVDF/HDTMA-modified clinoptilolite nanocomposite membrane	7	98.5	—	44
PVDF ultrafiltration membrane modified with GO-PVA-NaAlg hydrogel	103	92–95	—	45
PVDF/GO/Ni	38.39	98	—	46
PVDF/Chitosan/CNT	85	>90%	—	47
SAGO@PVDF membrane	**450 at 30 psi**	**97–99**	**50(Na$_2$SO$_4$)**	**This work**

demonstrates that the SAGO@PVDF membrane efficiently rejects 96% and 99% for all dye molecules. Zeta potential measurements confirm that the membrane surface exhibits a negative charge, and MB and RB are cationic dyes; hence, adsorption is the main mechanism by which the MB and RB dye is rejected. Electrostatic repulsion, on the other hand, caused the SAGO@PVDF membrane to reject CR and MO. Our research indicates that the SAGO@PVDF membranes had outstanding dye separation efficiency. Fig. 11c–f displays the feed and permeate solutions' UV-vis spectra following dye rejection.

The UV-visible spectra analysis of the permeate solutions revealed the absence of absorption maxima peaks associated with the specific dye foulants, namely MB (at 292 and 664 nm), CR (at 342 and 498 nm), RB (at 284, 306, 354, and 550 nm), and MO (at 273 and 464 nm). This observation indicates that the SAGO@PVDF membranes effectively removed both cationic and anionic dyes, demonstrating efficient dye removal capabilities. The membrane was highly reusable, as evidenced by the fact that it retained a rejection efficiency of >89% even after ten consecutive cycles (Fig. 11b). These results suggest that the SAGO@PVDF films have outstanding dye rejection and recycling performance.

An internal Sterlitech dead-end setup was used to measure the ion rejection performance of the manufactured SAGO@PVDF membranes. Na$_2$SO$_4$ and NaCl feed solutions with 1000 ppm concentrations each were used. The performance of the negatively charged membranes was comparable to that of the similarly charged NF membranes, where salt rejection occurred in the sequence Na$_2$SO$_4$ > NaCl (Fig. 12). Nearly 27% of NaCl and about 48% of Na$_2$SO$_4$ were rejected by the membranes. Size sieving and the Donnan exclusion principle work together to provide a reasonable explanation for such effective rejection. The presence of GO can reduce the effective pore size of the membrane, enabling more efficient sieving of salt ions based on their size. Additionally, the incorporation of GO can introduce functional groups that enhance the Donnan exclusion effect. However, as SO$_4^{2-}$ experiences more electrostatic repulsion than chloride ions do, the sulfate retention is significantly higher than the chlorides, which can be attributed to superior retention. Although, the salt rejection efficiency of SAGO@PVDF was low, indicating that the membrane is not effectively removing salts from the solutions. This could be due to defects in the membrane, an insufficient membrane thickness, or clogging or fouling of the membrane pores.

The key to successfully deploying GO-based membranes from practical standby is mechanical stability. According to the literature, GO-based membranes were unstable in various conditions, including acidic and alkaline media. Therefore, the stability of the SAGO@PVDF membranes was evaluated by submerging them for 60 days each in HCl (pH 2), deionized water (pH 7), and NaOH (pH 12) solutions. Surprisingly, the SAGO@PVDF membrane showed no cracks or leaching in an aqueous media with various pHs, indicating exceptional stability. After 60 days of immersion in acidic, neutral, and alkaline solutions, the cross-sectional SEM morphology of the SAGO@PVDF membrane showed network-like morphology retained (Fig. S2†). The exceptional stability of the SAGO@PVDF membrane offers numerous potentials for nanofiltration under various challenging operational situations.[42]

The SAGO@PVDF membrane demonstrated superior performance selectivity compared to other membranes reported in the literature. Table 1 presents a comparative study primarily focusing on dye rejection performances, highlighting that most reported membranes exhibit relatively low rejection rates. In contrast, our SAGO@PVDF membrane shows significantly higher rejection activity. This study marks a significant advancement in the development of stable and cost-effective GO@PVDF-based membranes for water purification applications.

4 Conclusion

We conclude by presenting a straightforward method for fabricating shear-aligned GO@PVDF membranes with a distinctive shape and organized structure. In this study, GO nanosheet dispersion was used to synthesize GO@PVDF membranes with a highly orientated lamellar phase. Shear align nanostructured GO@PVDF membranes were used for dye rejection selectively. Due to its stronger electrostatic interaction or repulsion, the rejection process involves effective dye rejection, but the common salts % is significantly less at ambient temperature. This shear-aligned GO sheet offers a method for producing novel GO@PVDF membranes with easily adjustable compositions, highly orientated morphologies, and optimized performances. The final GO@PVDF membranes-maintained stability under 100 psi of transmembrane pressure for extended periods and reported a pure water flux that was close to 4–5 times lower than the neat PVDF membranes and higher than existing literature. Methyl Orange and Rhodamine B were used as model dye foulants, and over numerous operating cycles, the membranes displayed >96% rejection. The GO nanosheets were aligned during the mix matrix membrane

fabrication process. We discovered that this novel strategy significantly improved the separation performance. Other materials' performance was hampered by bottlenecks like leaching and stability that provides our system an advantage in total performance.

Data availability

The data supporting this article have been included in the manuscript and ESI.†

Conflicts of interest

The authors declare that they have no known competing financial interests or personal relationships that could have appeared to influence the work reported in this paper.

Acknowledgements

References

1 M. Sajid, S. M. Sajid Jillani, N. Baig and K. Alhooshani, Layered double hydroxide-modified membranes for water treatment: Recent advances and prospects, *Chemosphere*, 2022, **287**, 132140, DOI: 10.1016/j.chemosphere.2021.132140.

2 A. Q. Al-Gamal and T. A. Saleh, Design and manufacturing of a novel thin-film composite membrane based on polyamidoamine-grafted graphene nanosheets for water treatment, *J. Water Process Eng.*, 2022, **47**, 102770, DOI: 10.1016/j.jwpe.2022.102770.

3 F. Soomro, F. H. Memon, M. A. Khan, M. Iqbal, A. Ibrar, A. A. Memon, *et al.*, Ultrathin Graphene Oxide-Based Nanocomposite Membranes for Water Purification, *Membranes*, 2023, **13**(1), 64, DOI: 10.3390/membranes13010064.

4 N. Padmavathy, S. S. Behera, S. Pathan, L. Das Ghosh and S. Bose, Interlocked Graphene Oxide Provides Narrow Channels for Effective Water Desalination through Forward Osmosis, *ACS Appl. Mater. Interfaces*, 2019, **11**(7), 7566–7575, DOI: 10.1021/acsami.8b20598.

5 Z. Zhang, X. Xiao, Y. Zhou, L. Huang, Y. Wang, Q. Rong, *et al.*, Bioinspired Graphene Oxide Membranes with pH-Responsive Nanochannels for High-Performance Nanofiltration, *ACS Nano*, 2021, **15**(8), 13178–13187, DOI: 10.1021/acsnano.1c02719.

6 F. Jia, L. Yang, L. Sun, D. Yu, Y. Song, Y. Wang, *et al.*, Efficient separation of dyes using two-dimensional heterogeneous composite membranes, *Water Res.*, 2023, **247**, 120693, DOI: 10.1016/j.watres.2023.120693.

7 S. Sharif, K. S. Ahmad, F. H. Memon, F. Rehman, F. Soomro and K. H. Thebo, Functionalised graphene oxide-based nanofiltration membranes with enhanced molecular separation performance, *Mater. Res. Innovations*, 2022, **26**(6), 373–381, DOI: 10.1080/14328917.2021.2006907.

8 Y. Zhang, H. Wang, W. Wang, Z. Zhou, J. Huang, F. Yang, *et al.*, Engineering covalent organic framework membranes for efficient ionic/molecular separations, *Matter*, 2024, **7**(4), 1406–1439, DOI: 10.1016/j.matt.2024.01.028.

9 H. Huang, Z. Song, N. Wei, L. Shi, Y. Mao, Y. Ying, *et al.*, Ultrafast viscous water flow through nanostrand-channelled graphene oxide membranes, *Nat. Commun.*, 2013, **4**(1), 2979, DOI: 10.1038/ncomms3979.

10 P. Sun, M. Zhu, K. Wang, M. Zhong, J. Wei, D. Wu, *et al.*, Selective Ion Penetration of Graphene Oxide Membranes, *ACS Nano*, 2013, **7**(1), 428–437, DOI: 10.1021/nn304471w.

11 K. H. Thebo, X. Qian, Q. Zhang, L. Chen, H.-M. Cheng and W. Ren, Highly stable graphene-oxide-based membranes with superior permeability, *Nat. Commun.*, 2018, **9**(1), 1486, DOI: 10.1038/s41467-018-03919-0.

12 A. Ali, F. Rehman, M. Ali Khan, F. H. Memon, F. Soomro, M. Iqbal, *et al.*, Functionalized Graphene Oxide-Based Lamellar Membranes with Tunable Nanochannels for Ionic and Molecular Separation, *ACS Omega*, 2022, **7**(36), 32410–32417, DOI: 10.1021/acsomega.2c03907.

13 A. H. Jatoi, K. H. Kim, M. A. Khan, F. H. Memon, M. Iqbal, D. Janwery, *et al.*, Functionalized graphene oxide-based lamellar membranes for organic solvent nanofiltration applications, *RSC Adv.*, 2023, **13**(19), 12695–12702, DOI: 10.1039/D3RA00223C.

14 M.-U.-N. Khilji, A. A. Otho, R. Memon, A. Khalid, M. Kazi, A. Hyder, *et al.*, Facile Fabrication of a Free-Standing Magnesium Oxide-Graphene Oxide Functionalized Membrane: A Robust and Efficient Material for the Removal of Pollutants from Aqueous Matrices, *Anal. Lett.*, 2023, 1–18, DOI: 10.1080/00032719.2023.2284841.

15 I. Mahar, F. K. Mahar, N. Mahar, A. A. Memon, A. A. A. Pirzado, Z. Khatri, *et al.*, Fabrication and characterization of MXene/carbon composite-based nanofibers (MXene/CNFs) membrane: An efficient adsorbent material for removal of Pb+2 and As+3 ions from water, *Chem. Eng. Res. Des.*, 2023, **191**, 462–471, DOI: 10.1016/j.cherd.2023.02.005.

16 W. Wang, C. Wang, Y. Zhang, H. Xu and L. Shao, Highly positively-charged membrane enabled by a competitive reaction for efficient Li+/Mg2+ separation, *Sep. Purif. Technol.*, 2024, **330**, 125428, DOI: 10.1016/j.seppur.2023.125428.

17 J. Guo, Y. Zhang, F. Yang, B. B. Mamba, J. Ma, L. Shao, *et al.*, Ultra-Permeable Dual-Mechanism-Driven Graphene Oxide Framework Membranes for Precision Ion Separations, *Angew. Chem., Int. Ed.*, 2023, **62**(23), e202302931, DOI: 10.1002/anie.202302931.

18 D. D. Kachhadiya and Z. V. P. Murthy, Preparation and characterization of ZIF-8 and ZIF-67 engineered PVDF mixed-matrix membranes: stability enhancement in

pervaporation study, *Environ. Sci.: Water Res. Technol.*, 2023, **9**(5), 1502–1517, DOI: **10.1039/D3EW00027C**.

19 S. Zhang, X. Wu, Z. Huang, X. Tang, H. Zheng and Z. Xie, The selective sieving role of nanosheets in the development of advanced membranes for water treatment: Comparison and performance enhancement of different nanosheets, *Sep. Purif. Technol.*, 2021, **273**, 118996, DOI: **10.1016/j.seppur.2021.118996**.

20 X. Liu, H. Yuan, C. Wang, S. Zhang, L. Zhang, X. Liu, *et al.*, A novel PVDF/PFSA-g-GO ultrafiltration membrane with enhanced permeation and antifouling performances, *Sep. Purif. Technol.*, 2020, **233**, 116038, DOI: **10.1016/j.seppur.2019.116038**.

21 D. D. Kachhadiya and Z. V. P. Murthy, Graphene oxide modified CuBTC incorporated PVDF membranes for saltwater desalination via pervaporation, *Sep. Purif. Technol.*, 2022, **290**, 120888, DOI: **10.1016/j.seppur.2022.120888**.

22 A. Ghobadi Moghadam and A. Hemmati, Improved water purification by PVDF ultrafiltration membrane modified with GO-PVA-NaAlg hydrogel, *Sci. Rep.*, 2023, **13**(1), 8076, DOI: **10.1038/s41598-023-35027-5**.

23 Y. Zhang, L. Liu and F. Yang, A novel conductive membrane with RGO/PVDF coated on carbon fiber cloth for fouling reduction with electric field in separating polyacrylamide, *J. Appl. Polym. Sci.*, 2016, **133**(26), 1–9, DOI: **10.1002/app.43597**.

24 L. M. Camacho, T. A. Pinion and S. O. Olatunji, Behavior of mixed-matrix graphene oxide – Polysulfone membranes in the process of direct contact membrane distillation, *Sep. Purif. Technol.*, 2020, **240**, 116645, DOI: **10.1016/j.seppur.2020.116645**.

25 G. Mao, T. Liu, Y. Chen, X. Gao, J. Qin, H. Zhou, *et al.*, Polyamide@GO microporous membrane with enhanced permeability for the molecular sieving of nitrogen over VOC, *J. Membr. Sci.*, 2022, **652**, 120443, DOI: **10.1016/j.memsci.2022.120443**.

26 A. Rahimi and H. Mahdavi, Zwitterionic-functionalized GO/PVDF nanocomposite membranes with improved anti-fouling properties, *J. Water Process Eng.*, 2019, **32**, 100960, DOI: **10.1016/j.jwpe.2019.100960**.

27 F. Rehman, F. H. Memon, Z. Bhatti, M. Iqbal, F. Soomro, A. Ali, *et al.*, Graphene-based composite membranes for isotope separation: challenges and opportunities, *Rev. Inorg. Chem.*, 2022, **42**(4), 327–336, DOI: **10.1515/revic-2021-0035**.

28 F. Soomro, A. Ali, S. Ullah, M. Iqbal, T. Alshahrani, F. Khan, *et al.*, Highly Efficient Arginine Intercalated Graphene Oxide Composite Membranes for Water Desalination, *Langmuir*, 2023, **39**(50), 18447–18457, DOI: **10.1021/acs.langmuir.3c02699**.

29 C. Liu, J. Shen, C. Z. Liao, K. W. K. Yeung and S. C. Tjong, Novel electrospun polyvinylidene fluoride-graphene oxide-silver nanocomposite membranes with protein and bacterial antifouling characteristics, *eXPRESS Polym. Lett.*, 2018, **12**(4), 365–382, DOI: **10.3144/expresspolymlett.2018.31**.

30 L. Sun, D. Yu, Z. Juan, Y. Wang, Y. Wang, M. J. Kipper, *et al.*, pH-Responsive graphene oxide/poly (methacrylic acid) hybrid nanofiltration membrane performance for water treatment, *J. Environ. Chem. Eng.*, 2023, **11**(6), 111157, DOI: **10.1016/j.jece.2023.111157**.

31 A. Hyder, A. Ali, A. Khalid, A. Nadeem, M. A. Khan, A. W. Memon, *et al.*, Supramolecular Structural-Based Graphene Oxide Lamellar Membrane for Removing Environmental Pollutants from Wastewater, *Ind. Eng. Chem. Res.*, 2023, **62**(49), 21335–21346, DOI: **10.1021/acs.iecr.3c03260**.

32 D. Yu, L. Sun, Y. Zhang, Y. Song, C. Jia, Y. Wang, *et al.*, Two-dimensional graphene oxide/MXene lamellar membrane cross-linked by urea with adjustable interlayer spacing for efficient dye rejection and ion sieving, *Chem. Eng. J.*, 2024, **480**, 148009, DOI: **10.1016/j.cej.2023.148009**.

33 H. Yu, B. Zhang, C. Bulin, R. Li and R. Xing, High-efficient Synthesis of Graphene Oxide Based on Improved Hummers Method, *Sci. Rep.*, 2016, **6**(1), 36143, DOI: **10.1038/srep36143**.

34 Z. Xu, X. Yan, Z. Du, J. Li and F. Cheng, Effect of oxygenic groups on desalination performance improvement of graphene oxide-based membrane in membrane distillation, *Sep. Purif. Technol.*, 2020, **251**, 117304, DOI: **10.1016/j.seppur.2020.117304**.

35 W.-H. Zhang, M.-J. Yin, Q. Zhao, C.-G. Jin, N. Wang, S. Ji, *et al.*, Graphene oxide membranes with stable porous structure for ultrafast water transport, *Nat. Nanotechnol.*, 2021, **16**(3), 337–343, DOI: **10.1038/s41565-020-00833-9**.

36 S. A. Rahman, G. A. S. Haron, R. K. R. Kanasan and H. Hasbullah, Preliminary study on gas separation performance of flat sheet mixed matrix (PVDF/Zeolite), *IOP Conf. Ser.: Mater. Sci. Eng.*, 2018, **342**, 012073, DOI: **10.1088/1757-899X/342/1/012073**.

37 F. Baskoro, C.-B. Wong, S. R. Kumar, C.-W. Chang, C.-H. Chen, D. W. Chen, *et al.*, Graphene oxide-cation interaction: Inter-layer spacing and zeta potential changes in response to various salt solutions, *J. Membr. Sci.*, 2018, **554**, 253–263, DOI: **10.1016/j.memsci.2018.03.006**.

38 G. C. L. Wong, A. Lin, J. X. Tang, Y. Li, P. A. Janmey and C. R. Safinya, Lamellar Phase of Stacked Two-Dimensional Rafts of Actin Filaments, *Phys. Rev. Lett.*, 2003, **91**(1), 018103, DOI: **10.1103/PhysRevLett.91.018103**.

39 S. J. Mun, Y. H. Shim, G. W. Kim, S. H. Koo, H. Ahn, T. J. Shin, *et al.*, Tailored growth of graphene oxide liquid crystals with controlled polymer crystallization in GO-polymer composites, *Nanoscale*, 2021, **13**(4), 2720–2727, DOI: **10.1039/D0NR07858A**.

40 C. Shuai, Z. Zeng, Y. Yang, F. Qi, S. Peng, W. Yang, *et al.*, Graphene oxide assists polyvinylidene fluoride scaffold to reconstruct electrical microenvironment of bone tissue, *Mater. Des.*, 2020, **190**, 108564, DOI: **10.1016/j.matdes.2020.108564**.

41 A. Akbari, P. Sheath, S. T. Martin, D. B. Shinde, M. Shaibani, P. C. Banerjee, *et al.*, Large-area graphene-based nanofiltration membranes by shear alignment of discotic

nematic liquid crystals of graphene oxide, *Nat. Commun.*, 2016, **7**(1), 10891, DOI: **10.1038/ncomms10891**.

42 Z. Zhang, X. Xiao, Y. Zhou, L. Huang, Y. Wang, Q. Rong, *et al.*, Bioinspired Graphene Oxide Membranes with pH-Responsive Nanochannels for High-Performance Nanofiltration, *ACS Nano*, 2021, **15**(8), 13178–13187, DOI: **10.1021/acsnano.1c02719**.

43 R. Mohamat, A. B. Suriani, A. Mohamed, M. H. D. Muqoyyanah Othman, R. Rohani and T. Soga, Effect of Surfactants' Tail Number on the PVDF/GO/TiO 2-Based Nanofiltration Membrane for Dye Rejection and Antifouling Performance Improvement, *Int. J. Environ. Res.*, 2021, **15**, 149–161.

44 S. M. Hosseinifard, M. A. Aroon and B. Dahrazma, Application of PVDF/HDTMA-modified clinoptilolite nanocomposite membranes in removal of reactive dye from aqueous solution, *Sep. Purif. Technol.*, 2020, **251**, 117294, DOI: **10.1016/j.seppur.2020.117294**.

45 A. Ghobadi Moghadam and A. Hemmati, Improved water purification by PVDF ultrafiltration membrane modified with GO-PVA-NaAlg hydrogel, *Sci. Rep.*, 2023, **13**(1), 8076.

46 Y. Zhao, W. Yu, R. Li, Y. Xu, Y. Liu, T. Sun, *et al.*, Electric field endowing the conductive polyvinylidene fluoride (PVDF)-graphene oxide (GO)-nickel (Ni) membrane with high-efficient performance for dye wastewater treatment, *Appl. Surf. Sci.*, 2019, **483**, 1006–1016, DOI: **10.1016/j.apsusc.2019.04.054**.

47 J. Zhao, H. Liu, P. Xue, S. Tian, S. Sun and X. Lv, Highly-efficient PVDF adsorptive membrane filtration based on chitosan@CNTs-COOH simultaneous removal of anionic and cationic dyes, *Carbohydr. Polym.*, 2021, **274**, 118664, DOI: **10.1016/j.carbpol.2021.118664**.